V. ACKNOWLEDGMENTS

One of us (C.P.B.) is grateful to the administration of the Oak Ridge National Laboratory, who made their facilities available for the completion of this work, and to Dr. R. L. Graham for a private communication on Ho^{166}. It is a pleasure to acknowledge our thanks to Dr. T. A. Pond for making available a copy of the dissertation of Dr. W. A. W. Mehlhop.

PHYSICAL REVIEW VOLUME 120, NUMBER 4 NOVEMBER 15, 1960

Photoneutron Cross Sections of Cobalt and Manganese*

P. A. FLOURNOY, R. S. TICKLE, AND W. D. WHITEHEAD
University of Virginia, Charlottesville, Virginia

(Received June 15, 1960)

The total photoneutron yields of Mn^{55} and Co^{59} have been measured from threshold to approximately 30 Mev. Analysis of these data using the Leiss-Penfold matrix indicates that the cross sections for both elements show a splitting in the giant resonance region in accord with the predictions of the classical hydrodynamic model. The Mn^{55} peaks occur at energies of 16.8±0.25 Mev and 19.75±0.25 Mev corresponding to cross sections of 90 mb and 77 mb, respectively. Co^{59} maxima occur at 16.75±0.25 Mev and 18.75±0.25 Mev with cross sections of 109 mb and 92 mb. The cross sections $\sigma(\gamma,n)+\sigma(\gamma,2n)+\sigma(\gamma,np)+\cdots$ integrated to 25 Mev are 627 Mev-mb for Mn^{55} and 709 Mev-mb for Co^{59}. Breit-Wigner resonance lines were fitted to both cross sections and the intrinsic quadrupole moments determined from these fits are +0.78±0.10 barn for manganese and +0.76±0.11 barn for cobalt.

INTRODUCTION

As initially pointed out by Okamoto[1] and Danos,[2] if the classical hydrodynamic model of the nucleus affords a reasonable description of the nuclear photoeffect, one might expect, for strongly deformed nuclei, the giant resonance to be split into two separate resolvable resonances. The detailed calculations as performed by Danos[3] show that over the range of nuclear deformations, the splitting of the energy eigenvalues is accurately given by

$$\frac{\omega_b}{\omega_a}=0.911\frac{a}{b}+0.089, \tag{1}$$

where ω_a and ω_b refer to the resonance energies associated with the axes a and b of the spheroid chosen to represent the nuclear shape, a being the axis of rotational symmetry. If an eccentricity ϵ is defined as $\epsilon R^2=a^2-b^2$, where R is the radius of a sphere of equal volume $R^3=R_0{}^3A$, the intrinsic quadrupole moment of a spheroid with uniform charge distribution can be written as

$$Q_0=\tfrac{2}{5}R_0{}^2\epsilon ZA^{\frac{2}{3}}. \tag{2}$$

In an effort to substantiate the predictions by Okamoto and Danos, the initial experiments[4–6] were conducted on rare earth elements having large intrinsic quadrupole moments. Recently, Spicer[7] has pointed out that the splitting of the giant resonance of deformed nuclei into two components should be readily observable in the region $9\leq Z\leq 30$. Deformations in this region are comparable to those of rare earth nuclei. In addition, Spicer has re-examined the published cross sections for a number of nuclei of $9\leq Z\leq 30$ and interpreted the results as showing a splitting of the resonance consistent with the hydrodynamic model.

Using the published values of Q_0, the intrinsic quadrupole moment, obtained from microwave spectroscopy or Coulomb excitation, Spicer suggests five other nuclei in the chosen atomic number range in which a splitting of the giant resonance should be clearly observable.

Two of these suggested elements, cobalt and manganese, have been selected and closely examined as to the detailed shape of the total neutron production cross section in the giant resonance region.

EXPERIMENTAL PROCEDURE

Figure 1 is a schematic diagram of the synchrotron area. The x-ray beam is collimated to $\frac{7}{8}$ inch at the sample position by an eight-inch lead collimator located 80 cm from the tungsten target. The center of the neutron house was approximately two and one-half meters from x-ray source.

Photoneutrons are detected by BF_3 counters embedded in a paraffin cube. A thorough description of this method has been published by Halpern.[8] Eight counters were placed symmetrically on a cylinder of

* Supported by the Air Force Office of Scientific Research.
[1] K. Okamoto, Progr. Theoret. Phys. (Japan) **15**, 75 (1956).
[2] M. Danos, Bull. Am. Phys. Soc. **1**, 135 (1956).
[3] M. Danos, Nuclear Phys. **5**, 23 (1958).
[4] E. G. Fuller and M. S. Weiss, Phys. Rev. **112**, 560 (1958).
[5] B. M. Spicer, H. H. Thies, J. E. Baglin, and F. R. Allum, Australian J. Phys. **11**, 298 (1958).
[6] R. W. Parsons and L. Katz, Can. J. Phys. **37**, 809 (1959).
[7] R. M. Spicer, Australian J. Phys. **11**, 490 (1958).
[8] J. Halpern, A. Mann, and R. Nathans, Rev. Sci. Instr. **23**, 678 (1952).

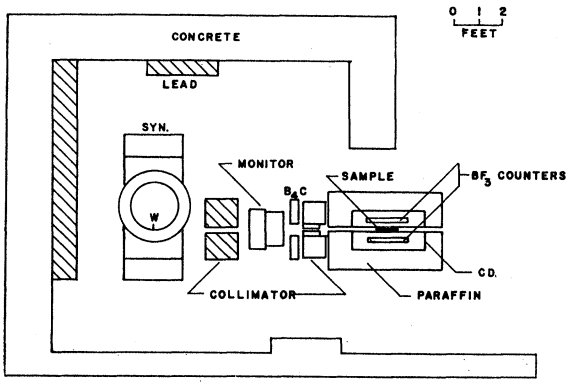

FIG. 1. Experimental arrangement.

13.5-cm radius within a two-foot paraffin cube. Extreme care was taken in shielding the counting matrix from neutrons originating outside the detector.

The eight BF_3 counters (N. Wood Counter Laboratory, 96% B^{10}, 40-cm Hg, 12 in. effective length) were separated into two channels with five 1-in. diameter counters in one channel and three 2 in. diameter counters in the other. Within each channel the counters were connected in parallel to a single cathode follower. The cathode follower outputs were then fed into two independent channels each consisting of a nonoverload amplifier, integral discriminator, gating circuit, and scaler. Both gates were set to open twenty microseconds after the x ray pulse and to remain open for seven hundred microseconds. To allow the counters to fully recover from the x ray burst before the gate opened and to avoid pile-up of neutron pulses, the counting rate in the most efficient channel was held under 80×64 counts per minute by decreasing the x ray yield at the higher energies. To the accuracy required, this rate was determined from a knowledge of counting rate versus beam intensity at several energies to be independent of intensity.

An absolute efficiency for neutrons was obtained by counting neutrons from a ten millicurie Ra-α-Be standard source. An efficiency of $2.88\pm0.15\%$ was found for the neutron detector for a point source located in the center of the detector. The variation of efficiency with position along the detector axis was also determined. The dependence of efficiency on neutron energy was not determined at this laboratory but is believed to be a constant for the energies present in this experiment.[9]

To obtain statistically significant cross-section values the photoneutron yield curves must be known to about 0.1%. This involves taking approximately a million counts at each yield point. The feasibility of such an experiment depends strongly on the stability of the electronics involved. Therefore, frequent checks were made of the neutron efficiency, gate delay, and gate length during the experiment.

[9] B. Rossi and H. Staub, *Ionization Chambers and Counters* (McGraw-Hill Book Company, Inc., New York, 1949), p. 152.

A duraluminum, parallel plate ionization chamber was used to monitor the x ray intensity. This chamber is an exact copy of chambers now in use in the Betatron Section of the National Bureau of Standards. Leiss *et al.*[10] have calibrated an identical chamber using a crystal spectrometer. Their results were used in analyzing the data reported in this paper. The charge produced within the ion chamber was collected on a Fast polystyrene film condenser, and the voltage across the condenser was measured with a Keithley Model 600 electrometer. The electrometer sensitivity was frequently checked throughout the run.

DATA ANALYSIS

The Leiss-Penfold method[11] was used to extract cross sections from the yield curves. The yield data (total count less background) were normalized to unit monitor response using the known response function for the ion chamber. The normalized yield was then used with the Leiss-Penfold matrix[12] to obtain values for the reduced cross section:

$$\Omega(K)=\frac{\sigma_{TN(K)}}{K}e^{-\mu(K)X}\times\frac{1}{L}\int_0^L F(X')e^{-\mu'(K)X'}dX',$$

where $\sigma_{TN}(K)$ is the total neutron cross section $\sigma(\gamma,n)+\sigma(\gamma,np)+2\sigma(\gamma,2n)$ at the photon energy K, $e^{-\mu(K)X}$ is an absorption correction for photons lost in the donut walls and ion chamber, $F(X')$ is the efficiency as a function of sample position, and $e^{-\mu(K)X'}$ is an absorption correction for photons absorbed within the sample. A one-Mev bin analysis was used to obtain values for the reduced cross section at integer Mev points. The Matrix was then shifted 0.5 Mev to obtain values at the remaining points. Statistical errors in the cross-section measurements were obtained by propagating the errors on the yield points through the inverse matrix.

MANGANESE

The yield data for manganese were taken at half Mev intervals in the energy region from 12 Mev to 25 Mev and thereafter at intervals of 1 Mev. Approximately twenty separate runs were made to define the yield function through the energy region 12–30 Mev. Errors on the yield data due to counting statistics alone were 0.5% at 14 Mev, improving to approximately 0.14% at 20 Mev. First differences of the normalized yields are shown in Fig. 2. The cross section extracted from the yield data is shown as the plotted points in Fig. 3. Included in these values are corrections for both photon absorption and neutron multiplicity arising from the $(\gamma,2n)$ reaction. Errors on these points were derived

[10] J. Leiss, J. Pruitt, and R. Schrack, National Bureau of Standards Report, NBS-6149, September, 1958 (unpublished).

[11] A. Penfold and J. Leiss, Phys. Rev. 114, 1332 (1959).

[12] A. Penfold and J. Leiss, Physics Research Laboratory Report, University of Illinois, Champaign, Illinois, 1958 (unpublished).

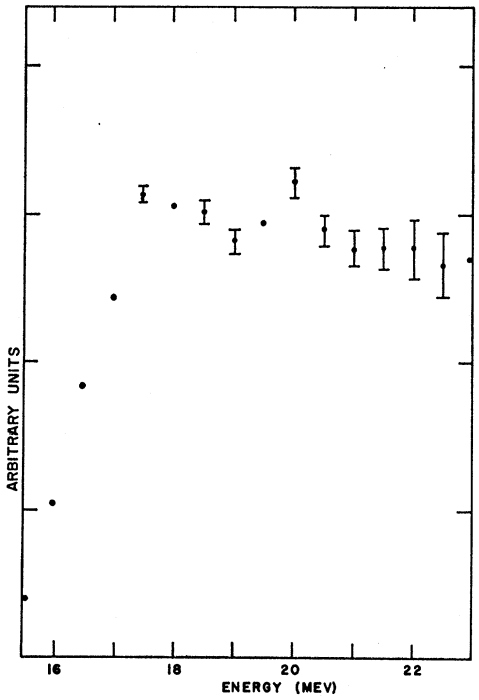

FIG. 2. First difference of manganese yield curve.

from the counting statistics. The integrated cross section to 25 Mev is 627 Mev-mb.

COBALT

Cobalt data were obtained at 0.5-Mev intervals from 12.0 Mev to 24.5 Mev and at 1.0-Mev intervals from 25.5 Mev to 35.5 Mev. The error in these measured values due to counting statistics are less than 0.1% from 17.0 to 20.5 Mev. Below 17.0 Mev the errors are larger, becoming 1% at 13.5 Mev. The first differences of the yield curve are shown in Fig. 4.

The total neutron cross section for cobalt was determined using the procedure outlined above. The data were then corrected for multiplicity of neutrons above the $(\gamma,2n)$ threshold of 18.6 Mev. The resulting cross section is shown as a function of incident photon energy in Fig. 5. The errors indicated are due to counting statistics alone. The integrated cross section from threshold to 25 Mev is 0.709 Mev-barns.

DISCUSSION OF RESULTS

The cross-section values for manganese and cobalt shown as the plotted points in Figs. 3 and 5 were corrected for neutron multiplicity above the $(\gamma,2n)$ threshold using the calculations based on the statistical model by Blatt and Weisskopf.[13] Θ, the temperature of the intermediate nucleus in the $(\gamma,2n)$ reaction, is defined as:

$$\Theta=(E_\gamma-E_0)^{\frac{1}{2}}/\sqrt{a},$$

where E_0 is the energy corresponding to the threshold of the (γ,n) reaction and a is a constant. In the computation of the multiplicity for both manganese and cobalt, the constant a was assigned the value 2 Mev^{-1}. Unfortunately, no experimental data are available on $(\gamma,2n)$ reactions in manganese and cobalt to afford an accurate multiplicity correction. Recent experimental data indicate that an appreciable fraction of the emitted neutrons may be due to "fast neutrons" which are emitted by a direct process without the formation of a compound state. This complicates the multiplicity correction in that calculations based on the statistical model will not apply to all the neutrons emitted above the $(\gamma,2n)$ threshold, tending to overestimate the required correction. In addition, neutrons of high energy

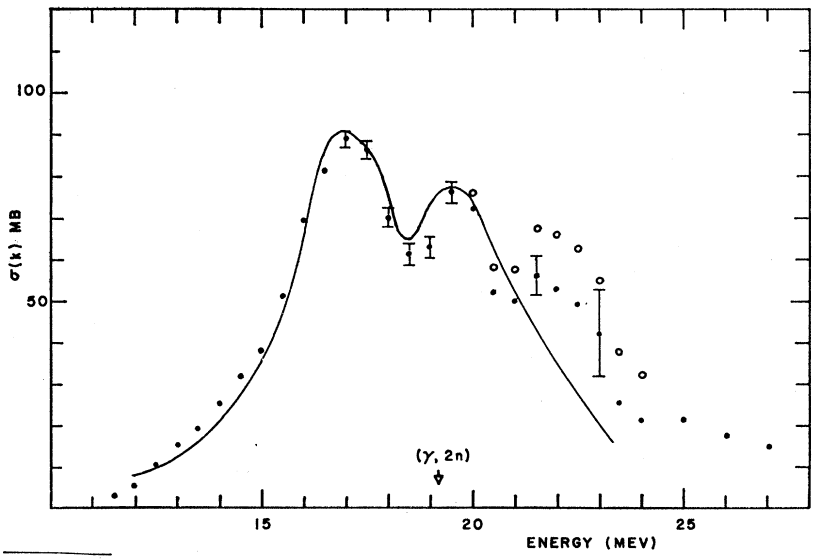

FIG. 3. Neutron cross section of manganese. Open circles represent uncorrected data. Closed circles represent data corrected for neutron multiplicity.

[13] J. M. Blatt and V. F. Weisskopf, *Theoretical Nuclear Physics* (John Wiley & Sons, Inc., New York, 1952), p. 379.

TABLE I. Parameters of Breit-Wigner fit to data.

Element	E_a (Mev)	Γ_a (Mev)	σ_a (mb)	E_b (Mev)	Γ_b (Mev)	σ_b (mb)	$\Gamma_b\sigma_b/\Gamma_a\sigma_a$
Manganese	16.8	2.7	70	19.75	4.0	64	1.35
Cobalt	16.5	2.0	78	19.0	4.0	78	2.00

may adversely affect the energy dependence of the detection system (assumed constant).

It should be pointed out that the absolute values assigned to the manganese and cobalt cross sections are estimated to be correct to within about fifteen percent. This uncertainty is due primarily to the use of the Schiff "integrated-over-angle" bremsstrahlung spectrum in the Leiss-Penfold matrix and the error assigned to the calibration of the ionization chamber. Also above the $(\gamma,2n)$ threshold, an additional source of error is present in the use of statistical theory to correct for the neutron multiplicity. While these factors preclude the accurate assignment of absolute values to the cross sections, it is felt that their effect on the relative shapes of the cross sections is sufficiently negligible to enable one to conclude the results indicate a splitting of the resonance.

The curves in Figs. 3 and 5 were fitted to the cross-section data and represent the sum of the two Breit-Wigner dispersion curves, i.e.,

$$\sigma=\frac{\sigma_a}{1+[2(E-E_a)/\Gamma_a]^2}+\frac{\sigma_b}{1+[2(E-E_b)/\Gamma_b]^2},$$

where the subscripts a and b refer to the low-energy peak and high-energy peak, respectively. Values of the parameters E_a, σ_a, Γ_a, E_b, σ_b, and Γ_b used to construct these curves are listed in Table I.

If the total photon absorption cross section is assumed to be well-approximated by the total neutron cross section measured in this experiment, the intrinsic quadrupole moment Q_0 may be computed on the basis of the hydrodynamic model for both manganese and cobalt using their respective ratios E_b/E_a and Eqs. (1) and (2). The resulting values of Q_0 are $+0.78\pm0.10$ barn for manganese and $+0.76\pm0.11$ barn for cobalt, using $R_0=1.2\times10^{-13}$ cm.

Parsons[14] has recently published results of a similar study of manganese and finds the intrinsic quadrupole

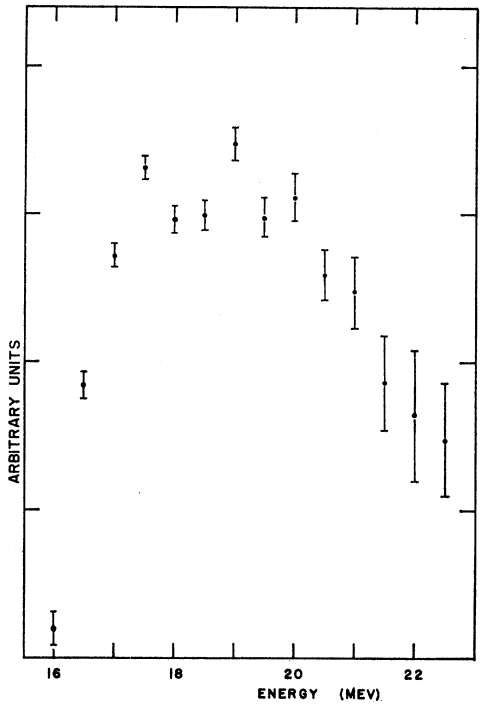

FIG. 4. First difference of cobalt yield curve.

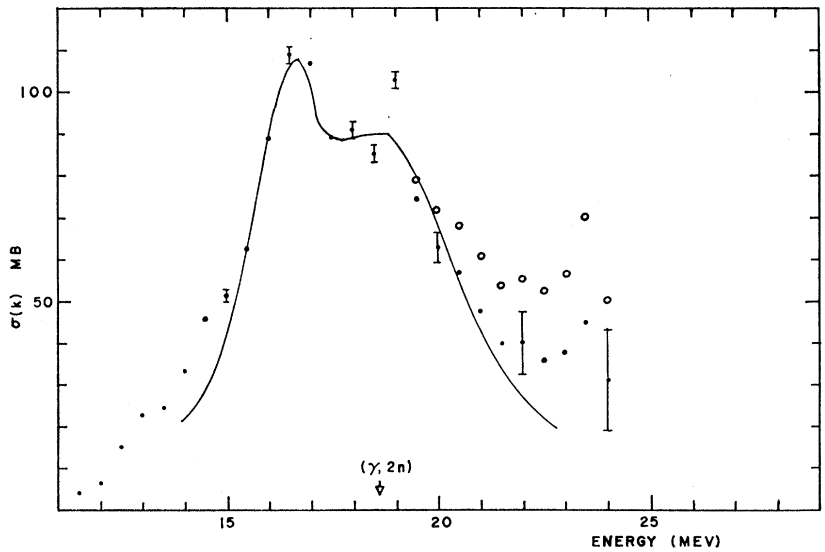

FIG. 5. Neutron cross section of cobalt. Open circles represent uncorrected data. Closed circles represent data corrected for neutron multiplicity.

[14] R. W. Parsons, Can. J. Phys. **37**, 1344 (1959).

TABLE II. Values are given for the nuclear eccentricity e and the intrinsic quadrupole moment Q_0.

Element	E_b/E_a	X	$e=(X-1)/X^{\frac{1}{3}}$	Q_0 (barns)
Mn[a]	1.18	1.19	0.18	$+0.78\pm0.10$
Co[a]	1.15	1.17	0.16	$+0.76\pm0.11$
Tb[b]	1.30	1.33	0.30	$+5.6\ \pm0.6$
Ta[b]	1.25	1.27	0.25	$+5.7\ \pm0.3$
Au[b]	1.06	1.07	0.07	$+1.6\ \pm0.6$

[a] Present data.
[b] E. G. Fuller and M. S. Weiss, reference 4.

moment to be 0.73 ± 0.14 barn. Considering the different methods of analysis and the statistical uncertainties involved, his results for manganese are in reasonable agreement with those presented here except for the absolute value assigned to the peak cross section; ours being some 20 mb larger.

Values of the spectroscopic quadrupole moment Q may be compared to the values of Q_0 obtained here if one assumes the validity of the collective nuclear rotation approximation[15] in which

$$Q_0=\frac{(I+1)(2I+3)}{I(2I-1)}Q,$$

where I is the ground-state spin.

For manganese, Murakawa[16] has obtained $Q=+0.4\pm0.2$ barn. Using this value, one obtains an intrinsic quadrupole moment of $+1.12\pm0.56$ barns. Likewise for cobalt, Murakawa[17] finds $Q=0.5\pm0.2$ barn from which $Q_0=1.07\pm0.43$ barns. These comparisons are of little value due to the rather large uncertainties associated with the spectroscopic quadrupole moments.

[15] A. Bohr and B. R. Mottelson, Kgl. Danske Videnskab. Selskab Mat—fys. Medd. **27**, No. 16 (1953).
[16] K. Murakawa, J. Phys. Soc. (Japan) **10**, 336 (1955).
[17] K. Murakawa and T. Kamei, Phys. Rev. **92**, 325 (1953).

Both Temmer and Heydenburg[18] and Mark, McClelland, and Goodman[19] have observed in Coulomb excitation experiments the $E2$ transition from the manganese ground state ($5/2^-$) to the excited state ($7/2^-$) at approximately 128 kev. Temmer and Heydenburg obtain a reduced transition probability (not corrected for internal conversion) of $B(E2)=0.075$ barn.[2] Assuming the $5/2^-$ to $7/2^-$ transition is within a rotation band, the $B(E2)$ value is then related to the intrinsic quadrupole moment in the following way[20]:

$$I\rightarrow I+1:\quad B(E2)=\frac{15}{16\pi}Q_0^2\frac{I}{(I+1)(I+2)},$$

where I is the nuclear spin of the ground state. Using $B(E2)=0.075$ barn,[2] a value of $Q_0=1.26\pm0.4$ barns is obtained, which is to be compared with the value $+0.78\pm0.10$ barn deduced from the present results.

Listed in Table II are values of the nuclear eccentricity, defined as $e=(a-b)/R$, where R is the radius of a sphere of equivalent volume. Defining $X=a/b$ and $R^3=ab^2$, the eccentricity becomes $e=(X-1)/X^{\frac{1}{3}}$. The values for tantalum, terbium, and gold were taken from the work by Fuller and Weiss.

ACKNOWLEDGMENTS

The authors wish to thank Dr. A. P. Batson, Dr. S. Berko, and Professor F. L. Hereford for their assistance in this experiment. They also appreciate assistance given in the actual data taking by Mr. R. Fast and Mr. G. Reinhardt. One of us (P. A. F.) wishes to acknowledge financial aid from a National Science Foundation Cooperative Fellowship.

[18] G. M. Temmer and N. P. Heydenburg, Phys. Rev. **104**, 967 (1956).
[19] H. Mark, C. McClelland, and C. Goodman, Phys. Rev. **98**, 1245 (1955).
[20] N. P. Heydenburg and G. M. Temmer, *Annual Review of Nuclear Science* (Annual Reviews, Inc., Palo Alto, 1956), Vol. 6, p. 107.